ICWMMN2006 Proceedings

A New Multiple-Frequency Millimeter Diplexer Using Microstrip Periodic-Stub

Yuemin Ning

Electronic Test & Measurement Technology National Laboratory, The 41st Institute of CETC

Qingdao 266555, P. R. China

E-mail: ymning@163.com

Abstract： In this paper, we introduce a three-port microstrip multi-frequency diplexer which can be used in phased-array transceiver system (PATS) and local multipoint distribution service (LMDS) that employ band-stop filters with open-circuited stubs for band selection and separation. The diplexer is designed to take 39.8, 42.4, 44.8 and 47.4 GHz into port 1 and to separate 39.8 and 44.8 GHz to port 2 and 42.4 and 47.4 GHz to port 3 with minimal dispersion. The insertion loss for each frequency varies from 0.4 to 1.2 dB and the return loss is better than 17.5 dB. The isolation between channels at the four frequencies is greater than 30 dB. Each passband created between adjacent stopbands has a bandwidth over 1.2 GHz. The microstrip diplexer is designed using periodic stubs that collectively have the advantages of low insertion loss, high isolation and rejection, wide-band performance on each channel, and easy fabrication. This type of diplexer has many applications in multi-frequency transceivers for millimeter communication systems.

Key words: diplexer, multiplexer, periodic filters.

Ⅰ. INTRODUCTION

Diplexers are three terminal devices that take two or more frequencies into one input port and separate them to two output ports. They are commonly used behind wide-band or multi-frequency antennas in transciever applications. Diplexers became widely studied in the early 1960’s by Matthaei et al. [1]-[2] and Wendel [3]. They studied microstrip diplexers that used bandpass/bandstop configurations as well as waveguide diplexers. In the late 1960’s, waveguides became widely used due to their very low insertion loss and high isolation. However, waveguides generally entail much more manufacturing complexity than planar etched microstrip diplexers. For this reason, microstrip diplexers have remained an active area of research. In the 1990’s, microstrip diplexers such as lowpass/bandpass [4] and ring diplexers [5] have gained notice [6].

The diplexer presented in this paper uses open-circuited periodic stubs as band-stop networks to provide both low loss and high isolation between the channels. The periodic stub geometry requires no gaps making the etching very reliable. The design provides the advantages of low loss and high isolation between channels and wide-band channel performance without the etching uncertainty found in gap-coupled filters. In 1996, Sheta et al. [7] used spurious harmonic modes for passbands in order to reduce the number of filters. The diplexer in this paper utilizes passbands formed between adjacent harmonic stopbands for size reduction and matching simplicity.

Ⅱ. THE DESIGN METHOD OF DIPLEXER

The diplexer schematic, as well as its individual filters shown in Fig. 1, was simulated using the full-wave electromagnetic simulator Ansoft HFSS. The diplexer consists of two filters which are connected by a T-junction. Each filter has ten sections of shunt stubs and each stub has a width of 0.2-mm. The space between each stub is 1.6-mm. The length of every stub in filter 1 which is composed of port 1 and port 2 is 10-mm. The length of every stub in filter 2 which is composed of port 1 and port 3 is 9.6-mm. The first stub in the left side of filter 1 and port 1 have a distance of 3.50-mm, The first stub in the left side of filter 2 and port 1 have a distance of 3.89-mm. The positioning of the filters from the T-junction was determined using Ansoft HFSS. These distances greatly affect the return loss or matching of the system, as well as the insertion loss. The whole diplexer was designed and fabricated on Al_2O_3 ceramic with a dielectric constant of 9.8 and thickness of 0.25-mm. All of the ports are terminated into 50 ohm. The input signals at port 1 (39.8, 42.4, 44.8, 47.4 GHz) are separated by the diplexer into two channels (39.8, 44.8 GHz into port 2 and 42.4, 47.4 GHz into port 3). The highest frequency in the Ansoft HFSS simulation was chosen to be 50 GHz and the gridding was set at 10 cells per wavelength.

The diplexer uses two periodic filter structures with open-circuited stubs to achieve the required stopbands. The centers of the stopbands occur when the lengths of the open-circuited stubs are at odd multiples of a quarter-wavelength. Low-loss passbands are formed between the adjacent stopbands. Each filter must be designed individually to yield the desired stopbands before combining the two as a diplexer. Stopbands can be shifted in frequency by changing the stub lengths. Making the stubs longer will shift the stopbands toward lower frequencies, as well as shorten the passbands. Making the stubs shorter will shift the stopbands toward higher frequencies and lengthen the passbands. The filter should be designed such that the lower possible harmonic stopbands are used to create the desired passbands since higher order harmonics will have more loss.

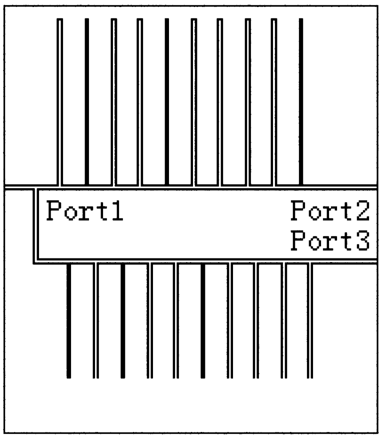

Fig.1 General diplexer schematic.

III. ANALYSIS OF THE MEASURED DATA

The diplexer's performance is plotted in Figs. 2–3. From the studying of the given data, we can find that filter 1 of Fig. 2-a passes 39.8 GHz between the six and seven harmonic stopbands and 44.8 GHz between the seven and eight harmonic stopbands. Similarly, filter 2 of Fig. 2-b passes 42.4 GHz between the six and seven harmonic stopbands and 47.4 GHz between the seven and eight harmonic stopbands. Fig. 2-c and 2-d give the S_{32} and S_{11} of the diplexer. From the simulation we can also find that although the positioning of the filters from the T-junction can greatly affect the return loss or the matching of the system, the isolations do not fluctuate much (<6 dB) with the variations of filter placement since the isolation created by the stopbands depends on the lengths of the open-circuited stubs. Each filter uses ten stubs to achieve more than 30 dB in isolation.

The results at 39.8, 42.4, 44.8, and 47.4 GHz are summarized in Table 1. The diplexer has very good passband insertion-loss performance due to the inherent low loss in the periodic filters. The measured insertion loss varies from 0.4 to 1.2 dB for the four frequencies. The isolation is extremely good and exceeds 30 dB for all four frequencies. Each of the passbands has very good bandwidth of around 1.2 GHz, as shown in Fig. 2. The return loss is better than 17.5 dB.

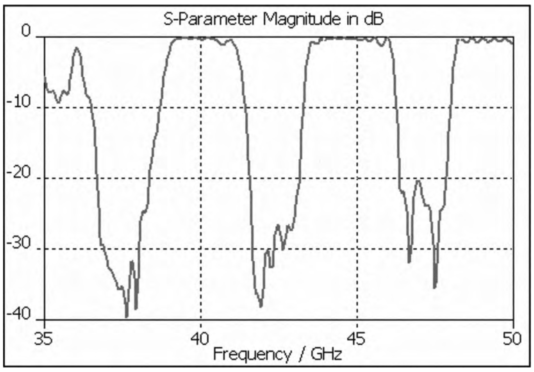

Fig.2-a S_{21} of the filter 1.

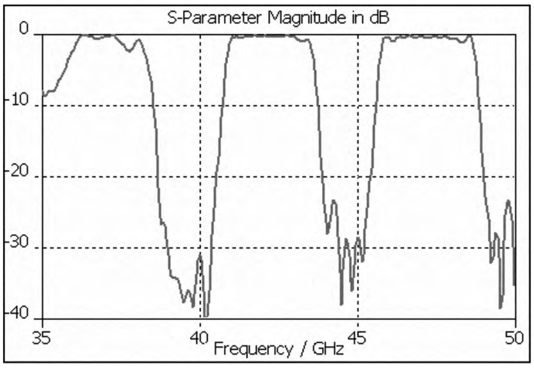

Fig.2-b S_{31} of the filter 2.

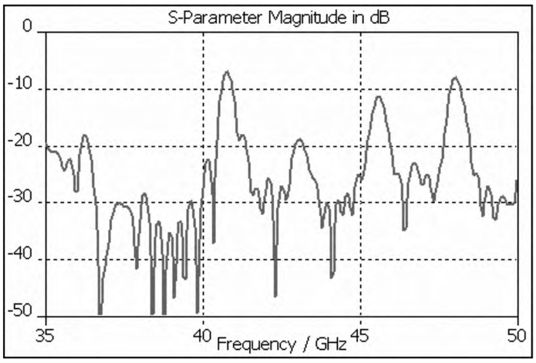

Fig.2-c S_{32} of the diplexer.

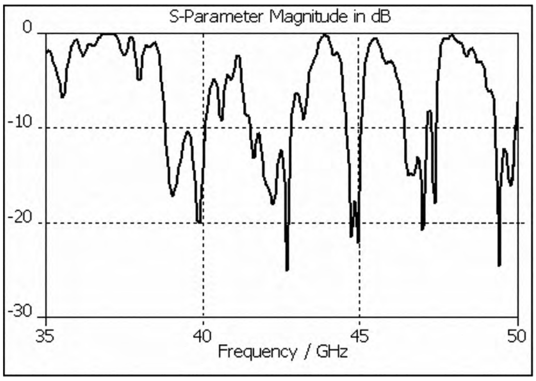

Fig.2-d S_{11} of the diplexer.

Table 1 The main parameter in four frequency.

Freq. / S para.	39.8 GHz	42.4 GHz	44.8 GHz	47.4 GHz
S_{11}(dB)	-18.5	-17.5	-20.7	-17.9
S_{21}(dB)	-0.4	-32.1	-0.5	-35.2
S_{31}(dB)	-38.3	-0.4	-28.4	-1.2
S_{32}(dB)	-43.2	-30.4	-31.7	-30.0

In order to minimize dispersion, the signal time delay of the frequencies of interest must be equal [8]. The energy at 39.8 and 44.8 GHz must flow from port 1 and reach port 2 at approximately the same time. Likewise, the energy at 42.4 and 47.4 GHz must flow from port 1 and reach port 3 at about the same time. Fig.3 shows the time delay for both channels of the diplexer.

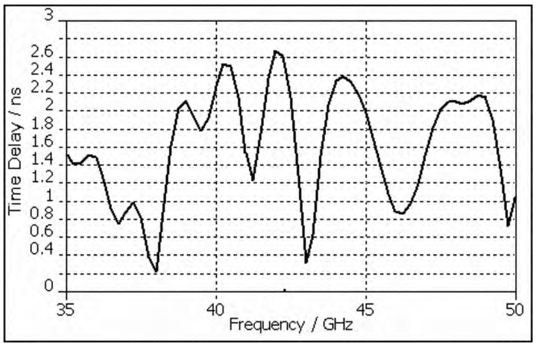

Fig.3-a Time delay for filter 1 (from port 1 to port 2).

From port 1 to 2, 39.8 and 44.8 GHz have time delays of 2.01 and 2.09 ns, respectively. Similarly, from ports 1 to 3, 42.4 and 47.4 GHz have time delays of 1.84 and 1.61 ns, respectively. The passbands containing 39.8, 42.4, 44.8, and 47.4 GHz have uniform time delay varying from around 1.55 to 2.21 ns. This constant time delay for the passbands is caused by the imaginary portion of the propagation constant being an almost linear function of frequency. This results in minimal dispersion.

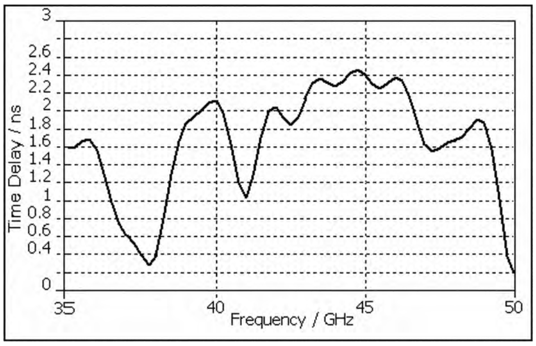

Fig.3–b Time delay for filter 2 (from port 1 to port 3).

Ⅳ. CONCLUSIONS

The simulated and measured data matches extremely well. Ansoft HFSS predicts the diplexer's behavior very well. The use of the periodic stub architecture allows many resonant sections to be used to achieve high isolation while maintaining low-loss performance and minimal dispersion. This diplexer is used for transmitting 39.8 and 44.8 GHz and receiving 42.4 and 47.4 GHz or vise versa. The filter could be built on a higher dielectric substrate for size reduction. The diplexer is very easy to manufacture and results are extremely reproducible because no coupling gaps are required.

ACKNOWLEDGMENT

The paper is subsidized by the fund of national base investigation (FNBI) and the author also would like to thank Jinglong YU, Communication University of China, for fabricating the microstrip circuits and measuring the performance of the diplexer.

REFERENCES

[1] Matthaei G, Young L, and Jones E M T. Microwave Filters Impedance-Matching Networks and Coupling Structures [M]. New York, McGraw-Hill, 1964.

[2] Matthaei G. and Cristal E G. "Multiplexer channel-separating units using interdigital and parallel-coupled filters". IEEE Trans. Microwave Theory Tech., 1965, vol.13, p.328–334.

[3] Wendel R J. "Printed-circuit complementary filters for narrow bandwidth multiplexers". IEEE Trans. Microwave Theory Tech., 1968, vol.16, p.147–157.

[4] Capstick M H. "Microstrip lowpass–bandpass diplexer topology". Electron. Lett., 1999, vol.35,p.1958–1960.

[5] Czawka G. "A new ring microstrip diplexer". Microwaves Radar Conf., 1998, vol. 2, p. 518–522.

[6] Henryk G. "Microwave diplexer with direct coupled filters". Microwaves Radar Conf., 1998, vol.2, p. 620–623.

[7] Sheta A F, Coupez J P, Tanne G, Toutain S, and Blot J P, "Miniature microstrip stepped impedance resonator bandpass filters and diplexers for mobile communications". IEEE MTT-S Int. Microwave Symp. 1996, vol. 2, p. 607–610.

[8] Pozar D M. Microwave Engineering [M]. New York, John Wiley & Sons, 1998.

Design procedure for multioctave combline-filter multiplexers

S. A. Alseyab, Ph.D., Mem. I.E.E.E., and Prof. J.D. Rhodes, C.Eng., Fel.I.E.E.E., M.I.E.E.

Indexing terms: Filters, Multiplexers

Abstract: A new general design procedure is presented for multioctave multiplexers having any number of combline channel filters satisfying an equiripple response, with an arbitrary number of resonators, bandwidths, and interchannel spacings. The design procedure is developed for bandpass combline filters connected in series at a common junction for broadband applications. Commencing with the expression for element values of a doubly-terminated-bandpass prototype combline filter satisfying an equiripple response, the multiplexer design procedure modifies the elements in the nearer half to the common junction of each channel filter and preserves a match at the two points of perfect transmission closest to the band edges of each channel filter, while taking into account the frequency dependence across each channel. Examples of several multiplexers are given indicating that the design process is valid for a wide variety of specifications and gives very good results as demonstrated by the computer analysis of multiplexer examples and by the experimental example of a combline-filter diplexer constructed in a coaxial form of realisation.

1 Introduction

Broadband multiplexers, often spanning several octaves, are most frequently used in electronic warfare applications. They allow several signals to share a common broadband device, usually an antenna. Most of the multiplexers developed during the late sixties and early seventies used high-pass/low-pass or band-pass/band-stop diplexer configurations in cascade. Elliptic prototypes were used to obtain sharp cutoffs and maintain a certain rejection level over very broadband e.g. Reference 1. These devices have the disadvantage of being both difficult and expensive to design. In addition, the number of filters used for a given number of channels is high e.g. at least five filters for a triplexer. The main reason that the cascade of diplexers approach has been used is because, during those years, it seemed too difficult to cover a multioctave band with a common-junction bandpass multiplexer. Meanwhile, the broadband combline filter has been undergoing continual improvement. It can nowadays be constructed in a straightforward manner from the theoretical prototype with bandwidths approaching 100%, stopband performance can exceed several times the upper passband edge with no spurious response. The insertion loss and the v.s.w.r. in the passband can be kept quite low even for a relatively high number of resonator filters. Therefore attention in recent years has focused on using combline bandpass filters to achieve smaller-size lower-cost bandpass common-junction multiplexers.

A design method for combline-filter multiplexers was presented more than a decade ago by Matthaei and Cristal.[2] Their design equations are based upon narrow-band approximation and the filters should be either singly terminated or foreshortened doubly terminated. The junction design consists of high-impedance lines connected between the junction and the input resonators of the separated channel filters. However, the method was limited to a total frequency range of the order of one octave due to the narrow band approximation used in the design of individual channels. More recently LaTourette[3-5] presented several attempts to design multioctave combline-filter multiplexers. His main concern was focused on obtaining a minimum-susceptance band-pass channel filter by adding extra circuits to the original nonminimum-susceptance singly-terminated combline structure in order to achieve a parallel-connected common-junction multiplexer. Although these attempts have resulted in particularly successful devices, their design are still lacking in generality and in most cases the additional circuits make the manufacturing and the adjusting of these devices much more expensive and difficult to achieve.

This paper presents a new general design procedure for multioctave combline-filter multiplexers having any number of Chebyshev channel filters, with arbitrary numbers of resonators, bandwidths and interchannel spacings. This procedure may be considered as an extension of the work introduced in a previous paper[6] which describes a multiplexer design procedure for narrowband applications. It commences with the element values of a doubly-terminated-bandpass prototype combline filter satisfying an equiripple response which is obtained from recently-introduced design equations.[7] These individual channel filters are connected at a common junction. The multiplexer design procedure modifies the elements in the nearer half to the common junction of each channel filter and, as in a similar manner to that given in Reference 6, it preserves a complete match at the two points of perfect transmission closest to the passband edges of each channel filter.

This paper begins by reviewing the combline-filter design equations introduced recently by Rhodes.[7] Although these equations are approximate they have been adopted here because of their compactness and when used in a computerised multiplexer design method – as is the case here – they certainly require less computer time compared with the well-known exact design methods for combline filters.

Then the multioctave multiplexer design procedure is presented. The computer analyses of several multiplexers are shown. Finally, a design example of a combline-filter diplexer constructed in a coaxial form of realisation is given and its experimental insertion-loss and return-loss characteristics are established.

2 Design formulas for broadband combline filter

The multioctave combline-filter multiplexer design procedure commences from a lumped/distributed element

Paper 1066H, first received 25th February and in revised form 12th September 1980

Prof. Rhodes is, and Dr. Alseyab was formerly, with the Department of Electrical & Electronic Engineering, University of Leeds, Leeds LS2 9JT, England. Dr. Alseyab is now with the Department of Electrical Engineering, University of Basrah, Bashar, Iraq

0143–7097/80/06346 + 08 $01·50/0

doubly-terminated combline channel filter, operating in isolation, satisfying an equiripple passband amplitude response shown in Fig. 1 and given by[7]

$$I.L. = 10\log(1 + \epsilon^2 F_n^2(\omega)) \qquad (1)$$

where

$$F_n(\omega) = \cos\left[n\cos^{-1}\left\{\frac{\omega_1\tan(a\omega_1) + \omega_2\tan(a\omega_2) - 2\omega\tan(a\omega)}{\omega_2\tan(a\omega_2) - \omega_1\tan(a\omega_1)}\right\}\right.$$

$$\left. + \cos^{-1}\left\{\frac{\tan(a\omega_1)\tan(a\omega_2)(\omega_2 - \omega_1) + (\tan(a\omega_2) - \tan(a\omega_1)\,\omega\tan(a\omega)}{\tan(a\omega)(\omega_2\tan(a\omega_2) - \omega_1\tan(a\omega_1))}\right\}\right] \qquad (2)$$

ω_1 and ω_2 are the lower and upper bandedge frequencies n is number of resonators in the network shown in Fig. 2 whose lumped counterpart has $(2n - 1)$ transmission zeros at infinity and a single transmission zero at the origin.

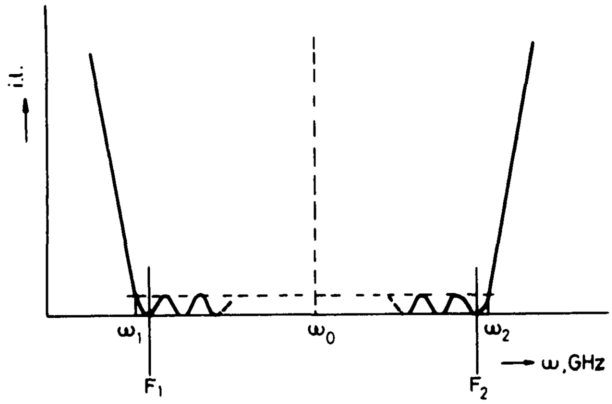

Fig. 1 *Insertion-loss response of combline filter*

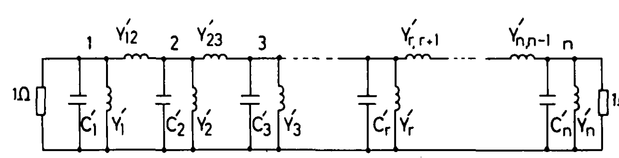

Fig. 2 *Equivalent network of doubly-terminated combline filter*

However, by extracting a negative-shunt short-circuited stub of characteristic admittance $(-Y'_{r,r+1})$ from every resonator in the network, an equivalent format consisting of resonators separated by frequency dependent admittance inverters with characteristic admittance $Y'_{r,r+1}\cot(a\omega)$ is obtained. Scaling all admittances by $\cot(a\omega)/\cot(a\omega_0)$, where ω_0 is the passband centre frequency) results in the network shown in Fig. 3, where the rth shunt resonator

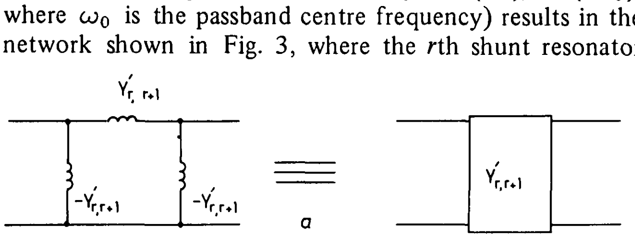

Fig. 3A *Equivalent network of inverter of characteristic admittance $Y'_{r,r+1}$*

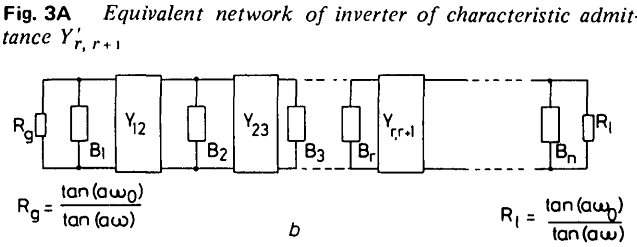

Fig. 3B *Scaled equivalent format of combline network*

possesses an admittance

$$B_r = j\{C_r\omega\tan(a\omega) - Y_r\} \qquad (3)$$

and the resonators are separated by ideal admittance inverters of characteristic admittance $Y_{r,r+1}$, but the terminating resistances become frequency dependents i.e.

$$R_g = R_l = \cot(a\omega)/\cot(a\omega_0) \qquad (4)$$

However, it has been shown by Rhodes,[7] that very good approximations of the design formulas for this prototype network can easily be obtained to satisfy bandwidth specifications of up to an octave using only the dominant term in $F_n(\omega)$ given in eqn. 2 such that

$$F_n(\omega) \simeq \cos\left[n\cos^{-1} x\right.$$

$$\left.\left\{\frac{\omega_1\tan(a\omega_1) + \omega_2\tan(a\omega_2) - 2\omega\tan(a\omega)}{\omega_2\tan(a\omega_2) - \omega_1\tan(a\omega_1)}\right\}\right] \qquad (5)$$

By comparing this prototype combline filter, which satisfies the equiripple response in the variable $\omega\tan(a\omega)$ given in eqn. 5, with the low-pass prototype satisfies a conventional Chebyshev response in the variable ω, having a passband $\omega = \pm 1$ and centre frequency at $\omega = 0$. The approximate centre frequency ω_0 of the combline is obtained when the argument of $F_n(\omega)$ is zero. Hence

$$2\omega_0\tan(a\omega_0) = \omega_1\tan(a\omega_1) + \omega_2\tan(a\omega_2) \qquad (6)$$

and the frequencies F_1 and F_2 where the perfect transmission occurs closest to the bandedges, can be obtained when the argument is $\pm\cos(\pi/2n)$, respectively, i.e.

$$\left.\frac{\omega_1\tan(a\omega_1) + \omega_2\tan(a\omega_2) - 2\omega\tan(a\omega)}{\omega_2\tan(a\omega_2) - \omega_1\tan(a\omega_1)}\right|_{\omega = F_1} =$$

$$= \cos(\pi/2n) \qquad (7)$$

and

$$\left.\frac{\omega_1\tan(a\omega) + \omega_2\tan(a\omega_2) - 2\omega\tan(a\omega)}{\omega_2\tan(a\omega_2) - \omega_1\tan(a\omega_1)}\right|_{\omega = F_2} =$$

$$= -\cos(\pi/2n) \qquad (8)$$

Hence, from eqn. 7

$$F_1\tan(aF_1) = \omega_1\tan(a\omega_1)\cos^2(\pi/4n) + \omega_2\tan(a\omega_2)\sin^2(\pi/4n) \qquad (9)$$

and from eqn. 8

$$F_2\tan(aF_2) = \omega_1\tan(a\omega_1)\sin^2(\pi/4n) + \omega_2\tan(a\omega_2)\cos^2(\pi/4n) \qquad (10)$$

However, the values of ω_0, F_1 and F_2 can be obtained by using one of the standard numerical techniques (e.g.

Newton-Raphson) in solving eqns. 6, 9 and 10 for given values of n, ω_1 and ω_2.

The derivation of the design formulas for the combline is based on preserving unity transmission with the correct overall phase shift in the auxiliary parameter $-j\eta$ or $j\eta$ at the frequencies F_1 and F_2, where η is as defined in eqn. 13. For broadband applications the $\cot(a\omega)/\cot(a\omega_0)$ frequency dependence of the terminating resistances R_l and R_g must be taken into account. Furthermore, the internal impedance level is allowed to vary and the sections of the network in question are only required to be image matched. Thus the overall transfer matrix of the network at F_1 is given by[7]

$$\prod_{r=1}^{n-1} \frac{1}{\sqrt{(\eta^2+S_r^2)(1+t_r^2)}} \times \begin{bmatrix} -\sqrt{\frac{Z_{1r}}{Z_{1r+1}}}(S_r+t_r) & j\sqrt{Z_{1r}Z_{1r+1}}\,(\eta-S_rt_r) \\ \frac{(\eta-S_rt_r}{\sqrt{Z_{1r}Z_{1r+1}}} & -\sqrt{\frac{Z_{1r+1}}{Z_{1r}}}(S_r+\eta t_1) \end{bmatrix} \tag{11}$$

and the overall transfer matrix of the network at F_2 is given by

$$\prod_{r=1}^{n-1} \frac{1}{\sqrt{(\eta^2+S_r^2)(1+t_r^2)}} \times \begin{bmatrix} \sqrt{\frac{Z_{2r}}{Z_{2r+1}}}(S_r-\eta t_r) & j\sqrt{Z_{2r}Z_{2r+1}}\,(\eta+S_rt_r) \\ j\frac{(\eta+S_rt_r}{\sqrt{Z_{2r}Z_{2r+1}}} & \sqrt{\frac{Z_{2r+1}}{Z_{2r}}}(S_r-\eta t_r) \end{bmatrix} \tag{12}$$

where the quantities in these two equations are defined as follows:

$$\eta = \sinh\left\{\frac{1}{h}\sinh^{-1}\left(\frac{1}{\epsilon}\right)\right\} \tag{13}$$

t_r is a phase correcting factor introduced to preserve the all-pass characteristic of the channel filter at F_1 and F_2 (to be determined)

Z_{1r} and Z_{2r} are the image impedances of rth section of the channel filter and required to be different at F_1 and F_2

$S_r = \sin(r\pi/n)$

Employing the same argument presented in Reference 6, matrix eqn. 11 yields the characteristic admittance of the inverter.

$$Y_{r,r+1} = \frac{\sqrt{(\eta^2+S_r)(1+t_r^2)}}{\sqrt{Z_{1r}Z_{1r+1}}(\eta-S_rt_r} \qquad r = 1 \to \frac{n}{2} \tag{14}$$

and the admittance of the rth shunt resonator between the inverters $Y_{r-1,r}$ and $Y_{r,r+1}$ is

$$C_rF_1\tan(aF_1) - Y_r = \frac{-1}{Z_{1r}}\left\{\frac{(S_r+\eta t_r)}{(\eta-S_rt_r)} + \frac{(S_{r-1}+\eta t_{r-1})}{(\eta-S_{r-1}t_{r-1})}\right\} \qquad r = 1 \to \frac{n}{2} \tag{15}$$

Similarly, from matrix eqn. 12

$$Y_{r,r+1} = \frac{\sqrt{(\eta^2+S_r)(1+t_r^2)}}{\sqrt{Z_{2r}Z_{2r+1}}\,(\eta+S_rt_r)} \qquad r = 1 \to \frac{n}{2} \tag{16}$$

and

$$C_rF_2\tan(aF_2) - Y_r = \frac{1}{Z_{2r}}\left\{\frac{(S_r-\eta t_r)}{(\eta+S_rt_r)} + \frac{(S_{r-1}-\eta t_{r-1})}{(\eta+S_{r-1}t_{r-1})}\right\} \qquad r = 1 \to \frac{n}{2} \tag{17}$$

To match into the terminating resistances at F_1 and F_2, the internal image impedance of section $r = 1$ must be respectively

$$Z_{11} = \frac{\tan(a\omega_0)}{\tan(aF_1)} \tag{18a}$$

and

$$Z_{21} = \frac{\tan(a\omega_0)}{\tan(aF_2)} \tag{18b}$$

Since the network is symmetrical, then

$$Z_{1n} = Z_{11} \tag{19a}$$

$$Z_{2n} = Z_{21} \tag{19b}$$

and the impedance variation level can be approximately expressed by[6, 7]

$$Z_{1r+1} = (Z_{1r})^{1/4} \qquad r = 1 \to \frac{n}{2} \tag{20a}$$

$$Z_{2r+1} = (Z_{2r})^{1/4} \qquad r = 1 \to \frac{n}{2} \tag{20b}$$

On the other hand, since $Y_{r,r+1}$ is the characteristic admittance of a frequency-independent inverter, then from eqns. 14 and 16 it results in

$$R_{0r+1} = \frac{1}{R_{0r}}\left(\frac{\eta+S_rt_r}{\eta-S_rt_r}\right)^2 \tag{21}$$

where

$$R_{0r} = \frac{Z_{1r}}{Z_{2r}} = \frac{\tan(aF_2)}{\tan(aF_1)} \tag{22}$$

and consequently

$$R_{0r+1} = (R_{0r})^{1/4} \qquad r = 1 \to \frac{n}{2} \tag{23}$$

Rearranging eqn. 21, t_r can be expressed by

$$t_r = \frac{\eta}{S_r}\left(\frac{\sqrt{R_{0r}R_{0r+1}}-1}{\sqrt{R_{0r}R_{0r+1}}+1}\right) \qquad r = 1 \to \frac{n}{2} \tag{24}$$

Having obtained all of the values on the right hand side of eqns. 15 and 17, they can then be solved to give the values of C_r and Y_r as

$$C_r = \frac{A_{0r}/Z_{1r} + B_{0r}/Z_{2r}}{F_2\tan(aF_2) - F_1\tan(aF_1)} \qquad r = 1 \to \frac{n}{2} \tag{25}$$

and

$$Y_r = C_rF_1\tan(aF_1) + A_{0r}/Z_{1r} \qquad r = 1 \to \frac{n}{2} \tag{26}$$

where

$$A_{0r} = \left(\frac{S_r + \eta t_r}{\eta - S_r t_r} + \frac{S_{r-1} + \eta t_{r-1}}{\eta - S_{r-1} t_{r-1}}\right) \quad (27a)$$

and

$$B_{0r} = \left(\frac{S_r - \eta t_r}{\eta + S_r t_r} + \frac{S_{r-1} - \eta t_{r-1}}{\eta + S_{r-1} t_{r-1}}\right) \quad (27b)$$

3 Multiplexer design procedure

As mentioned earlier, this design procedure is for multi-octave combline filter multiplexers having any number (L) of Chebyshev channel filters, with arbitrary numbers of resonators, bandwidths and interchannel spacings. The design procedure is developed for bandpass combline filters connected in series at a common junction. It commences from the lumped/distributed element values of a doubly-terminated prototype. These element values are obtained from the formulas given in the last Section for the given values of: number of resonators n_i ($i = 1 \to L$), passband edge frequencies ω_{1i} and ω_{2i}, passband minimum return loss, and the quarter wavelength frequency f_0.

The design principles used here are similar to those used in Reference 6. But only the elements in the nearer half to the common junction at each channel filter are modified here, taking into account the frequency variation across each channel and the interaction due to other channels.

A perfect transmission is preserved with the correct overall phase in the auxiliary variable η at the two points of perfect transmission (F_{1i} and F_{2i}) closest to the passband edges of each channel. However, when channel j ($j = 1, 2, 3, \ldots, L$) is modified, the remaining channels i ($i = 1, 2, 3, \ldots, \neq j, \ldots, L$) are replaced by their input impedances calculated at F_{1j} and F_{2j} to create frequency-dependent complex loads at one end which are connected in series with the generator resistance having values of

$$Z_{3j} = \tan(a\omega_{0j})/\tan(aF_{1j}) \quad (28a)$$

and

$$Z_{4j} = \tan(a\omega_{0j})/\tan(aF_{2j}) \quad (28b)$$

at F_{1j} and F_{2j} respectively. The equivalent circuit of the multiplexer is shown in Fig. 4, where

$$R_{1t}(F_{1j}) = \sum_{i \neq j}^{L} R_{1i}(F_{1j}) \tan(a\omega_{0i})/\tan(a\omega_{0j}) \quad (29a)$$

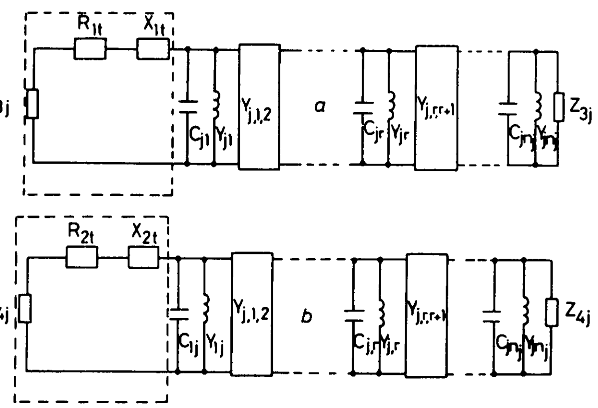

Fig. 4 *Equivalent circuit of combline channel-filter multiplexer with series-connected load*

a At $\omega = F_{1j}$ $\quad Z_{3j} = \tan(a\omega_{0j})/\tan(aF_{1j})$
b At $\omega = F_{2j}$ $\quad Z_{4j} = \tan(a\omega_{0j})/\tan(aF_{2j})$

$$X_{1t}(F_{1j}) = \sum_{i \neq j}^{L} X_{1i}(F_{1j}) \tan(a\omega_{0i})/\tan(a\omega_{0j}) \quad (29b)$$

$$R_{2t}(F_{2j}) = \sum_{i \neq j}^{L} R_{2i}(F_{2j}) \tan(a\omega_{0i})/\tan(a\omega_{0j}) \quad (29c)$$

and

$$X_{2t}(F_{2j}) = \sum_{i \neq j}^{L} X_{2i}(F_{2j}) \tan(a\omega_{0i})/\tan(a\omega_{0j}) \quad (29d)$$

$R_{1t}(F_{1j})$ and $R_{2t}(F_{2j})$ are the sums of the real parts of the input impedances of the individual channels evaluated at F_{1j} and F_{2j}, respectively, and $X_{1t}(F_{1j})$ and $X_{2t}(F_{2j})$ are the sums of the imaginary parts of the input impedances of the individual channels evaluated at F_{1j} and F_{2j}, respectively. The real and imaginary parts of the input impedance of each individual channel may be given by:

$$R_{1i}(F_{1j}) = Z_{5i}(A_{1i}D_{1i} + B_{1i}C_{1i})/\{D_{1i}^2 + (Z_{5i}C_{1i})^2\} \quad (30a)$$

$$X_{1i}(F_{ij}) = (B_{1i}D_{1i} - Z_{5i}^2 A_{1i}C_{1i})/\{D_{1i}^2 + (Z_{5i}C_{1i})^2\} \quad (30b)$$

$$R_{2i}(F_{2j}) = Z_{6i}(A_{2i}D_{2i} + B_{2i}C_{2i})/\{D_{2i}^2 + (Z_{6i}C_{2i})^2\} \quad (30c)$$

and

$$X_{2i}(F_{2j}) = (B_{2i}D_{2i} - Z_{6i}^2 A_{2i}C_{2i})/\{D_{2i}^2 + (Z_{6i}C_{2i})^2\} \quad (30d)$$

where

$$Z_{5i} = \tan(a\omega_{0i})/\tan(aF_{1j}) \quad (31a)$$

$$Z_{6i} = \tan(a\omega_{0i})/\tan(aF_{2j}) \quad (31b)$$

ω_{0i} is the passband centre frequency of channel i, and A_{1i}, B_{1i}, C_{1i} and D_{1i} are the entries of the overall transfer matrix of channel i calculated at F_{1j}. A_{2i}, B_{2i}, C_{2i} and D_{2i} are the same entries calculated at F_{2j}.

For convenience, the series-connected load from the common junction side to channel j is replaced by its shunt equivalent circuit as shown in Fig. 5 where $G_{1t}(F_{1j})$ and $G_{2t}(F_{2j})$ are the real parts, and $B_{1t}(F_{1j})$ and $B_{2t}(F_{2j})$ are the imaginary parts. Hence, they are given by

$$G_{1t}(F_{1j}) = \{Z_{3j} + R_{1t}(F_{1j})\}/[\{Z_{3j} + R_{1t}(F_{1j})\}^2 + X_{1t}^2(F_{1j})] \quad (32a)$$

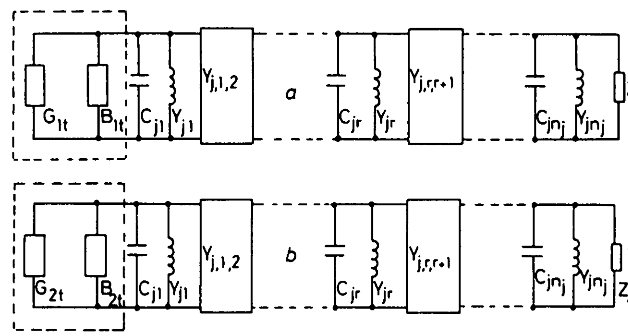

Fig. 5 *Equivalent circuit of combline-channel filter multiplexer with parallel-connected load*

a At $\omega = F_{1j}$ $\quad Z_{3j} = \tan(a\omega_{0j})/\tan(aF_{1j})$
b At $\omega = F_{2j}$ $\quad Z_{4j} = \tan(a\omega_{0j})/\tan(aF_{2j})$

$$B_{1t}(F_{1j}) = -X_{1t}(F_{1j})/[\{Z_{3j}+R_{1t}(F_{ij})\}^2 + X_{1t}^2(F_{ij})] \quad (32b)$$

and

$$G_{2t}(F_{2j}) = \{Z_{4j}+R_{2t}(F_{2j})\}/[\{Z_{4j}+R_{2t}(F_{2j})\}^2 + X_{2t}^2(F_{2j})] \quad (32c)$$

$$B_{2t}(F_{2j}) = -X_{2t}(F_{2j})/[\{Z_{4j}+R_{2t}(F_{2j})\}^2 + X_{2t}^2(F_{2t})] \quad (32d)$$

Now consider the overall transfer matrices given in eqns. 11 and 12 representing channel j with all the remaining channels $i \neq j$ replaced by the shunt-connected load. Since the basic section of these matrices can be decomposed into a transfer matrix of a shunt resonator and an admittance inverter, hence the overall admittance of the rth shunt resonator obtained from matrix equation (eqn. 11) can be described by

$$C_{j,r}F_{ij}\tan(aF_{ij}) - Y_{j,r} = \frac{-1}{Z_{1j,r}}\left\{\frac{(S_{j,r}+\eta_j t_{j,r})}{\eta_j - S_{j,r}t_{j,r}} + \frac{(S_{j,r-1}+\eta_j t_{j,r-1})}{\eta_j - S_{j,r-1}t_{j,r-1}}\right\} \quad (33)$$

and the characteristic admittance of the inverter is given by

$$Y_{j,r,r+1} = \frac{\sqrt{(\eta_j^2 + S_{j,r})(1+t_{j,r}^2)}}{\sqrt{Z_{1j,r}Z_{1j,r+1}}\,(\eta_j - S_{j,r}t_{j,r})}$$

$$r = 1 \rightarrow \frac{n_j}{2} \quad (34)$$

Similarly from eqn. 12

$$C_{j,r}F_{2j}\tan(aF_{2j}) - Y_{j,r} = \frac{1}{Z_{2j,r}}\left\{\frac{(S_{j,r}-\eta_i t_{j,r})}{(\eta_j + S_{j,r}t_{j,r})} + \frac{(S_{j,r-1}-\eta_j t_{j,r-1})}{(\eta_j + S_{j,r-1}t_{j,r-1})}\right\} \quad (35)$$

and

$$Y_{j,r,r+1} = \frac{\sqrt{(\eta_j^2 + S_{j,r}^2)(1+t_{j,r}^2)}}{\sqrt{Z_{2j,r}Z_{2j,r+1}}\,(\eta_j + S_{j,r}t_{j,r})}$$

$$r = 1 \rightarrow \frac{n_j}{2} \quad (36)$$

Once again, since $Y_{j,r,r+1}$ is frequency independent then, from eqns. 34 and 36, the expression for $t_{j,r}$ can be written as

$$t_{j,r} = (\eta_j/S_{j,r})\left(\frac{\sqrt{R_{0j}R_{0j,r+1}}-1}{\sqrt{R_{0j}R_{0j,r+1}}+1}\right)$$

$$r = 1 \rightarrow \frac{n_j}{2} \quad (37)$$

where $t_{j,0} = 0$

$$R_{0j,r} = \frac{Z_{1j,r}}{Z_{2j,r}} \quad (38)$$

It has been found that the impedance level variation still follows the expression given in eqns. 20*a* and *b*. Furthermore, for all-pass behaviour in the auxiliary parameter for each channel at its critical frequencies F_{ij} and F_{2j}, the following relationships must be applied

$$Z_{1j,1} = 1/G_{1t}(F_{1j}) \quad (39a)$$

$$Z_{2j,1} = 1/G_{2t}(G_{2j}) \quad (39b)$$

and

$$R_{0j,1} = G_{2t}(F_{2j})/G_{1t}(F_{1j}) \quad (39c)$$

However, the modified values of the elements associated with the first resonator of channel j can be obtained by solving the following two equations for $C_{j,1}$ and $Y_{j,1}$

$$B_{1t}(F_{1j}) + C_{j,1}F_{1j}\tan(aF_{1j}) - Y_{j,1} = -A_{0j,1} \quad (40)$$

$$B_{2t}(F_{2j}) + C_{j,1}F_{2j}\tan(aF_{2j}) - Y_{j,1} = B_{0j,1} \quad (41)$$

resulting in

$$C_{j,1} = \{A_{0j,1} + B_{0j,1} + B_{1t}(F_{ij}) - B_{2t}(F_{2j})\}/\{F_{2j}\tan(aF_{2j}) - F_{1j}\tan(aF_{1j})\} \quad (42)$$

and

$$Y_{j,1} = C_{j,1}F_{1j}\tan(aF_{1j}) + A_{0j,1} + B_{1t}(F_{1j}) \quad (43)$$

where

$$A_{0j,1} = G_{1t}(F_{1j})(S_{j,1}+\eta_j t_{j,1})/(\eta_j - S_{j,1}t_{j,1}) \quad (44)$$

and

$$B_{0j,1} = G_{2t}(F_{2j})(S_{j,1}-\eta_j t_{j,1})/(\eta_j + S_{j,1}t_{j,1}) \quad (45)$$

The modified values of the elements associated with the remaining resonators in the nearer half to the common junction of channel j can be obtained by solving eqns. 34 and 36 for $C_{j,r}$ and $Y_{j,r}$ ($r = 1 \rightarrow n_j/2$) to give

$$C_{j,r} = \left(\frac{A_{0j,r}}{Z_{1j,r}} + \frac{B_{0j,r}}{Z_{2j,r}}\right)\Big/\{F_{2j}\tan(aF_{2j}) - F_{1j}\tan(aF_{1j})\} \quad (46)$$

and

$$Y_{j,r} = C_{j,r}F_{2j}\tan(aF_{2j}) - B_{0j,r}/Z_{2j,r} \quad (47)$$

where

$$A_{0j,r} = \frac{S_{j,r}+\eta_j t_{j,r}}{\eta_j - S_{j,r}t_{j,r}} + \frac{S_{j,r-1}+\eta_j t_{j,r-1}}{\eta_j - S_{j,r}t_{j,r-1}} \quad (48)$$

and

$$B_{0j,r} = \frac{S_{j,r}-\eta_j t_{j,r}}{\eta_j + S_{j,r}t_{j,r}} + \frac{S_{j,r-1}-\eta_j t_{j,r-1}}{\eta_j + S_{j,r-1}t_{j,r-1}} \quad (49)$$

The modified characteristic admittance $Y_{j,r,r+1}$ of the inverter can be obtained by using either of eqns. 34 or 36.

The values of the elements associated with the other half of each channel remain without change as in isolation.

A computer program has been written to perform the modification process. This process is then repeated channel by channel until all the element values converge to certain values and no further change is possible.

4 Prototype examples and computer analysis

The validity of this design procedure for multioctave combline-filter multiplexers is demonstrated by the computer analysis of several design examples for a wide variety of specifications as follows:

(i) A 5-channel multiplexer has been designed with each of its channels having 8 resonators, bandwidths of 1 GHz, and minimum return loss of 20 dB. The combline channel filters consist of lumped capacitors and short-circuited stubs. Each of these stubs is a quarter wavelength long at 15 GHz. The individual channel specifications and the modified element values are given in Table 1. The return-loss and insertion-loss characteristics are plotted in Figs. 6 and 7, respectively.

(ii) A triplexer has been designed with each of the 3 channels having 6 resonators, bandwidths of 2 GHz, and minimum return loss of 26 dB. The short-circuited stubs are quarter wavelength long at $f_0 = 20$ GHz. The individual channel specifications and the modified element values are given in Table 2. The return-loss and the insertion-loss characteristics are plotted in Figs. 8 and 9, respectively.

Table 1: Element values of 5-channel combline-filter multiplexer

	r	1	2	3	4	5	6	7	8
Channel 1									
$n_1 = 8$,	C_{1r}	6·15292	16·9766	26·6197	31·8151	31·9064	26·9409	18·0062	5·72712
$\omega_{11} = 1$,	Y_{1r}	1·32438	4·67732	7·10123	8·44703	8·4796	7·21645	5·08485	1·59616
$\omega_{12} = 2$	$Y_{1,r,r+1}$	1·19927	2·00606	2·57862	2·78418	2·59703	2·06586	1·38083	0
Channel 2									
$n_2 = 8$,	C_{2r}	3·53269	8·38213	12·7745	15·1522	15·1747	12·8509	8·58717	2·9376
$\omega_{21} = 2{\cdot}5$,	Y_{2r}	3·53633	8·58893	12·8967	15·264	15·2871	12·9752	8·80508	3·0048
$\omega_{22} = 3{\cdot}5$	$Y_{2,r,r+1}$	1·32225	2·05792	2·59524	2·78866	2·60489	2·08877	1·40436	0
Channel 3									
$n_3 = 8$,	C_{3r}	2·11281	5·10663	7·77753	9·22878	9·24611	7·8345	5·23597	1·81499
$\omega_{31} = 4$,	Y_{3r}	5·0425	12·1066	18·1972	21·5514	21·5867	18·3121	12·336	4·26759
$\omega_{32} = 5$	$Y_{3,r,r+1}$	1·32091	2·05472	2·5941	2·78834	2·60634	2·09304	1·40914	0
Channel 4									
$n_4 = 8$,	C_{4r}	1·28897	3·3158	5·06887	6·02742	6·04392	5·12214	3·42365	1·1919
$\omega_{41} = 5{\cdot}5$,	Y_{4r}	5·91935	14·8966	22·4531	26·6443	26·7067	22·6514	15·2233	5·2925
$\omega_{42} = 6{\cdot}5$	$Y_{4,r,r+1}$	1·2957	2·03933	2·58896	2·78695	2·60682	2·09447	1·41092	0
Channel 5									
$n_4 = 8$,	C_{5r}	0·400102	1·9617	3·23439	3·92308	3·96027	3·35653	2·24382	0·782341
$\omega_{51} = 7$,	Y_{5r}	3·56139	15·1568	24·6297	29·811	30·0801	25·5114	17·1332	5·96677
$\omega_{52} = 8$	$Y_{5,r,r+1}$	1·00144	1·90812	2·54606	2·77532	2·607	2·09502	1·41188	0

ω_{i1} and ω_{i2} are in GHz; $C_{ir}/2\pi \times 10^{-9}$ farads; Y_{ir} and $Y_{i,r,r+1}$ are in seimens; minimum return loss = 20 dB for all channels.

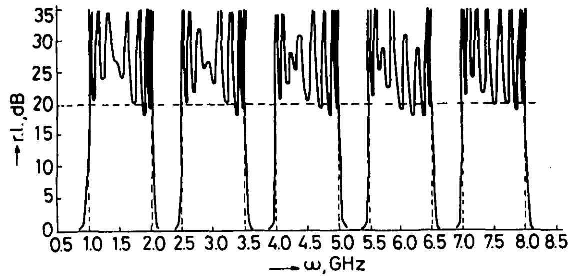

Fig. 6 *Return-loss response of 5-channel combline-filter multiplexer*

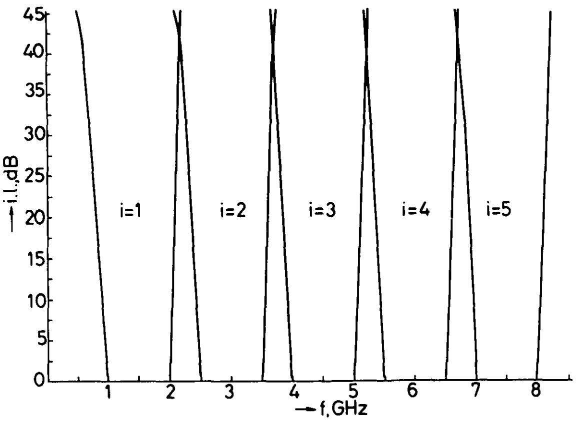

Fig. 7 *Insertion-loss characteristic of 5-channel combline-filter multiplexer*

Table 2: Element values of combline-filter triplexer

	r	1	2	3	4	5	6
Channel 1							
$n_1 = 6$,	C_{1r}	1·638657	4·09635	5·89134	5·97556	4·40932	1·4245
$\omega_{11} = 2$,	Y_{1r}	1·03293	3·49723	4·80309	4·90869	3·93744	1·31704
$\omega_{12} = 4$	$Y_{1r,r+1}$	1·0506	1·57961	1·80382	1·63519	1·25028	0
Channel 2							
$n_2 = 6$,	C_{2r}	0·886556	1·89948	2·63698	2·65737	1·95072	0·688487
$\omega_{21} = 5$,	Y_{2r}	2·92143	6·29414	8·44107	8·49499	6·41074	2·2872
$\omega_{22} = 7$	$Y_{2r,r+1}$	1·17441	1·62015	1·81514	1·65202	1·25809	0
Channel 3							
$n_3 = 6$,	C_{3r}	0·197274	0·934837	1·36585	1·40874	1·03374	0·370092
$\omega_{31} = 8$,	Y_{3r}	2·13856	7·75791	10·8825	11·1736	8·34211	3·00667
$\omega_{32} = 10$	$Y_{3r,r+1}$	0·966651	1·52993	1·78877	1·65498	1·26054	0

ω_{i1} and ω_{i2} are in GHz, $C_{ir}/2\pi \times 10^{-9}$ in farads; Y_{ir} and $Y_{ir,r+1}$ in seimens; minimum return loss = 26 dB.

Table 3: Element values of combline-filter diplexer

	r	1	2	3	4	5	6
Channel 1							
$n_1 = 6$,	C_{1r}	3·58442	9·78544	13·8054	13·9554	10·2167	3·73072
$\omega_{11} = 5$,	Y_{1r}	8·95655	25·3634	35·8444	36·2587	26·5866	9·70533
$\omega_{12} = 5{\cdot}5$	$Y_{1r,\,r+1}$	1·24406	1·88815	2·15027	1·93985	1·38577	0
Channel 2							
$n_2 = 6$,	C_{2r}	2·82269	8·24469	11·6271	11·7664	8·61422	3·14686
$\omega_{21} = 5{\cdot}7$,	Y_{2r}	10·0143	28·2639	39·686	40·1356	29·4217	10·7453
$\omega_{22} = 6{\cdot}2$	$Y_{2r,\,r+1}$	1·23932	1·88261	2·14853	1·93997	1·38592	0

Minimum return loss = 20 dB in both channels; $C_{ir}/2\pi \times 10^{-9}$ farads, and Y_{ir} and $Y_{ir,\,r+1}$ are in seimens; element values are for 1Ω terminating loads.

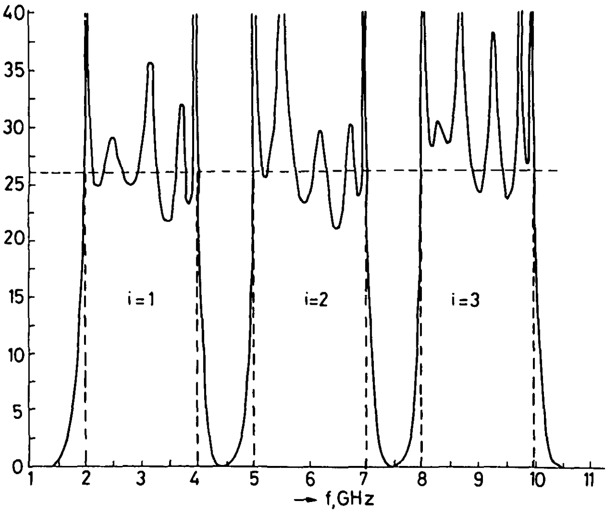

Fig. 8 *Return-loss characteristic of combline-filter triplexer*

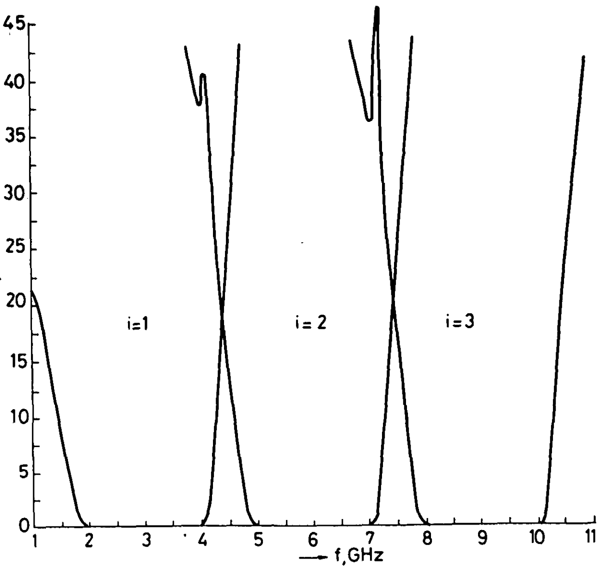

Fig. 9 *Insertion-loss characteristic of combline-filter triplexer*

5 Design and performance of combline-filter diplexer

The combline-filter diplexer has been designed with each channel having 6 resonators, bandwidths of 0·5 GHz, in-band minimum return loss equal 20 dB and the short-circuited stubs are quarter wavelength long at 18 GHz. The diplexer operates in 50Ω system. The bandedge frequencies and the element values are given in Table 3. The computer analysis of this diplexer showing the insertion-loss and return-loss characteristics is plotted in Fig. 10.

This diplexer was constructed in coaxial form of realis-

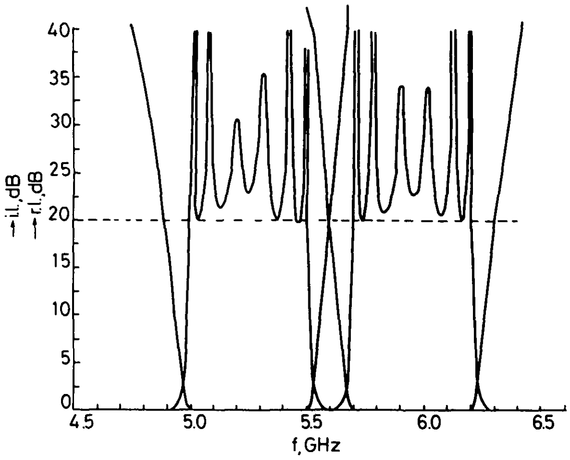

Fig. 10 *Insertion-loss and return-loss characteristics of combline-filter diplexer*

ation with all of the resonators in both channels having equal-diameter circular cylindrical rods. The design technique presented in Reference 8 has been used in obtaining the physical dimensions of the diplexer structure shown schematically in Fig. 11, its dimensions are obtained for the suitably chosen $d/b = 0{\cdot}4$ and $b = 0{\cdot}3$ in and given in Table 4 when each rod has a diameter $d = 0{\cdot}12$ in and since the length lr should be $\lambda/4$ at 18 GHz, thus $lr = 0{\cdot}146$ in.

The lumped capacitors have been realised by using screws. These screws from parallel-plate capacitances with the ends of the rods. However the distance D between the open end of the rods and the side wall of the metallic box is determined by

$$D = \epsilon_0 A/C \tag{50}$$

where:

ϵ_0 is the free space permittivity = $8{\cdot}842 \times 10^{-2}$ Fm^{-1}

A is the cross sectional area of the rod = $\pi d^2/4$

C is the smallest value of the capacitances given in Table 3 scaled to 50Ω termination and modified according to the successive scaling operation of the admittances to obtain equal-diameter-rods structure.[8] In this design example, the smallest value of C in Table 3 finally became equal to $2{\cdot}695 \times 10^{-13}$ F. Thus $D = 0{\cdot}009$ in.

The diplexer has been built and then tuned using a swept-frequency-reflectometer arrangement connected to the common port. The other ports were terminated with 50Ω loads. The experimental insertion-loss and common-port return-loss characteristics have been established and shown in Fig. 12.

6 Conclusions

A new general design procedure has been presented for multioctave combline-filter multiplexers. This procedure is

Table 4: Distances between the rods

Channel 1	Channel 2
(in)	(in)
S_{01} = 0·044	S_{01} = 0·046
S_{12} = 0·165	S_{12} = 0·174
S_{23} = 0·194	S_{23} = 0·204
S_{34} = 0·2	S_{34} = 0·207
S_{45} = 0·194	S_{45} = 0·204
S_{56} = 0·159	S_{56} = 0·171
S_{6T_1} = 0·047	S_{6T_2} = 0·048
S_{T_1W} = 0·045	S_{T_2W} = 0·042

former. Common-transformer diplexers have been used in practice for some time, but the theory behind the use of common-transfer coupling and the extension to multi-channels has not been verified until recently when Rhodes and Levy devoted a full Section in Reference 9 to the discussion of this topic.

The multiplexer design procedure presented in this paper has been programmed on a computer. An optimisation process has been used to modify the elements of each channel in turn and it has been found that the process normally converges if the insertion loss of the neighbouring channels cross over at greater than 3 dB. The very good results of this theory are demonstrated and confirmed by both the computer analysis of several multiplexers and by a practical diplexer.

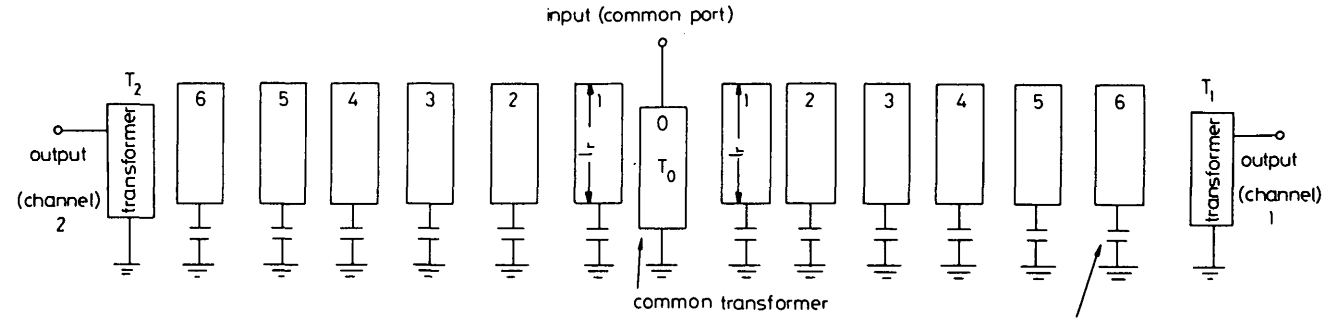

Fig. 11 *Symbolic representation of combline-filter diplexer*

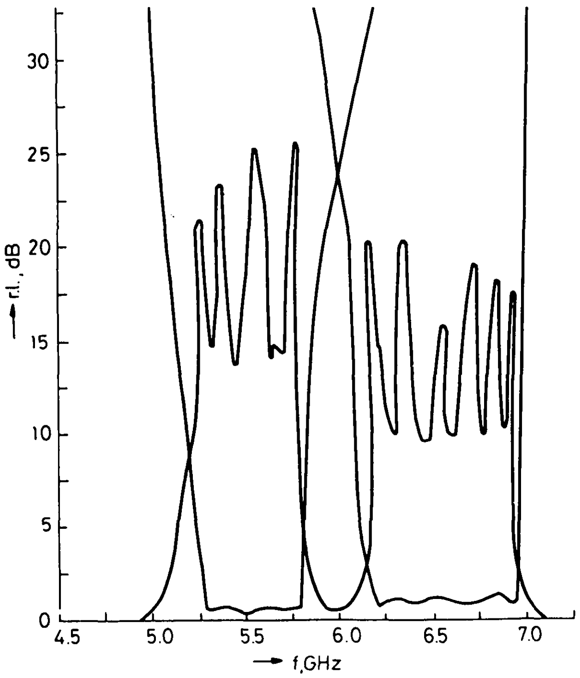

Fig. 12 *Experimental insertion-loss and return-loss characterictics of combline-filter diplexer*

based on the same principles of that introduced in Reference 6 and has all the merits, advantages and the approximations pointed there. In fact this procedure may be considered as an extension of the procedure introduced in Reference 6 to broadband applications. The individual combline channel filters are designed on the doubly-terminated bases using the recently introduced formulas.[7] Although these formulas are approximate, they nevertheless give excellent results up to an octave bandwidth. Furthermore, they are quite compact and can easily be programmed on a computer.

The individual channels are connected in series at a common junction without the addition of immittance compensation networks or dummy channels. However, the channels may be coupled by means of a common trans-

The practical diplexer has been realised in a coaxial form using air filled structure to give better temperature stability. It is believed that a good performance can be obtained also by using a suspended-substrate structure and the number of channels may increase at least to three. Further improvement could be obtained if the theory of the common transformer given in Reference 9 has been taken into account and the ground-plane spacing has been optimised to give the highest possible Q.

However, the practical devices designed according to the theory presented in this paper are less time consuming in the tuning and need no special arrangement as is the case for devices' designed on the singly terminated bases.

7 References

1 WENZEL, R.J.: 'Wideband high selectivity diplexers utilizing digital elliptic filters', *IEEE Trans.*, 1967, **MTT-15**, pp. 669–680
2 MATTHAEI, G.L., and CRISTAL, E.G.: 'Theory and design of diplexers and multiplexers', *in* YOUNG, L. (ed.): 'Advances in microwave' (Academic Press, 1967), pp. 237–326
3 La TOURETTE, P.M.: 'Multi-octave combline filter multiplexers'. IEEE MTT-S, International symposium digest, 1977, pp. 298–301
4 La TOURETTE, P.M.: 'Combline filter multiplexers', *Microwave J.*, 1977, **20**, pp. 55–59
5 La TOURETTE, P.M., and ROBERDS, J.L.: 'Extended junction combline multiplexers'. IEEE MTT-S, International symposium digest, 1978, pp. 214–216
6 RHODES, J.D., and ALSEYAB, S.A.: 'A design procedure for bandpass channel multiplexers connected at a common junction', *IEEE Trans.*, 1980, **MTT-28**, pp. 246–253
7 BRAYTON, L.O.: 'Modern Network Theory – an introduction' (Georgi Publishing Company, Switzerland, 1978)
8 RHODES, J.D., and ALSEYAB, S.A.: 'Simple design technique for TEM-networks having equal-diameter coupled circular cylindrical rods between parallel ground planes', *IEE J. Microwaves, Opt. & Acoust.*, 1979, **3** (4), pp. 142–146
9 RHODES, J.D., and LEVY, R.: 'A generalized multiplexer theory', *IEEE Trans.*, 1979, **MTT-27**, pp. 99–111